

# Thermal and Electrostatic Analyses of One Dimensional CFC Diagnostic Calorimeter for SPIDER Beam Characterisation

M. De Muri<sup>\*1,2</sup>, M. Dalla Palma<sup>1</sup>, P. Veltri<sup>1</sup>, A. Rizzolo<sup>1</sup>, N. Pomaro<sup>1</sup>, G. Seriani<sup>1</sup>

<sup>1</sup>Consorzio RFX, Euratom-ENEA association, Padova, Italy

<sup>2</sup>Dipartimento di Ingegneria Elettrica, Padova University, Italy

\* Dip. di Ingegneria Elettrica, via Gradenigo 6/A, 35131 Padova, interno 236, Italy, michela.demuri@igi.cnr.it

**Abstract:** Different types of simulations were dedicated to assess the possibility of constructing and making diagnostic use of an instrumented calorimeter devoted to the characterisation of the neutral beam injectors for the thermonuclear fusion experiment ITER. Transient non-linear thermal analyses (including radiation in some cases) have been done to investigate the behaviour of materials and the thermal response of the stainless steel frame. Electrostatic analyses have been done to choose a polarization value to avoid the effect of secondary electrons. From simulation results the requirements about the calorimeter have been deduced: one-dimensional CFC as the reference material, angled position, observation at the rear side, no active cooling, two axial distances, two positions, tiles electrically insulated, ten seconds pulse duration and 1200 seconds between pulses.

**Keywords:** Transient non-linear thermal analyses, electrostatic stationary analysis, instrumented calorimeter, NBI

## 1. Introduction

In the framework of activities for the design of the Padua Research on Injector Megavolt Accelerated (PRIMA) device, the beam source (SPIDER) has a key role in understanding the behaviour of sources before they are employed in the ITER Neutral Beam Injectors (NBIs) [1]. To this scope, SPIDER (Source for the Production of Ions of Deuterium Extracted from RF plasma) is equipped with several diagnostic systems and one of them is the Short-Time Retractable Instrumented Kalorimeter Experiment (STRIKE). It is a diagnostic intended to obtain a good knowledge of the beam features and it performs measurements about beam uniformity (negative ion current and power deposition), beam divergence and stripping losses. STRIKE is made of tiles directly intercepting the beam power and the heat deposited on the front side of the tiles is studied by thermal cameras observing

the back side. To preserve the image from one side to the other, special materials are required, exhibiting very large thermal conductivities in one direction with respect to the other two, like one-dimensional Carbon Fibre Carbon Composites.

### 1.1 Physical requirements

Among the characteristics of ITER Neutral Beam Injectors, beam uniformity within 10% is required. One of the aims of SPIDER is to provide a beam with a maximum 10% variation of the power load (beam current) across the beam. The primary scope of STRIKE is the assessment of beam uniformity. To this end, STRIKE is divided into tiles (called beamlet groups; passing through the accelerator the beam is divided into 1280 beamlets), reproducing the 4x4 symmetry of the beam source [2]. Moreover beam divergence and stripping losses are investigated.

Along the beam path different physical phenomena occur which make the measurements and their interpretation quite difficult. The divergence in a beam of charged particles is due to the repulsion force of the particles with the same charge and to the creation, in the accelerator, of neutrals not fully accelerated and no longer controlled by the electric field.

Stripping loss is due to collisions: impact of  $D^+$ ,  $D^-$  and  $D^0$  with the background gas produces ionisation in background gas and loss of electrons from negative beam particles. Stripping within the accelerator generates neutrals with lower energy, depending on the place where stripping occurs. In all cases electrons are generated. Around the calorimeter other phenomena take place: secondary electrons are emitted due to negative ion impact and, at high temperature, the material of the instrumented calorimeter sublimates forming a cloud in front of the calorimeter that can neutralize the  $D^-$  particles.

The measurement of the heat flux can be carried out by means of thermal cameras; their capabilities would however be hampered by the weak plasma formed in front of the surface of STRIKE which is hit by the beam: ionisation of low pressure background gas between the grounded grid and the calorimeter produces plasma. Plasma in its turn affects electric field distribution.

The STRIKE surface is subjected to a huge power load; to spread it over a larger area, while maintaining good measurement capabilities, the normal to the STRIKE surface shall be angled by 60° with respect to the beam direction. Moreover, because of the widely different thermal properties in different directions, the beam pulses at full power must be limited to a few seconds. Changing the measurement position of STRIKE allows a double characterisation of the beam, which results in the possibility of measuring the beam divergence. If also the electrical current reaching the tiles is measured, the stripping losses might be investigated; moreover electrical insulation of the tiles allows the study of the uniformity of the negative ion current.

## 2. Mathematical description

The general equation used is the following:

$$\frac{\partial T}{\partial \tau} = \frac{\lambda}{\rho c} \nabla^2 T + \sigma_0 S(T^4 - T_c^4)$$

Conduction and radiation are considered. In the case where only conduction is considered, at the end of heat load all faces of the tile are thermally insulated; the starting temperature is 300 K. In the case where also radiation (§3.6) is computed it is assumed that the face opposite to the one hit by the beam exchanges heat with a surface kept at room temperature (300 K), which is the starting temperature of the simulation. Indeed, since the rear side of the tile faces the vacuum vessel and the beam dump, which are at low temperature, it seems correct to assume a complete radiative heat exchange between the back side of the tile and the surface at 300 K, with view factor equal to 1. The radiative heat loss of the front side of the tile has been neglected, since the calorimeter panels mostly face each other, though not completely. Hence, it seems reasonable to think that the results represent an overestimate of the temperatures.

Spatial resolution of mesh in front and back surfaces is 1 mm, necessary to have a good and clear footprint of every beamlet.

## 3. Results presentation

### 3.1 Preliminary specification and feasibility study

The meaningfulness of electrical measurements depends on the capability to prevent secondary electrons extracted from a tile from being collected by another tile, in order to measure the beam current distribution. In the following it is assumed that the electrons exiting the accelerator do not reach the diagnostic calorimeter, whereas impact of  $D^-$ ,  $D^+$ ,  $D^0$  on calorimeter surface extracts secondary electrons, with energy of 3 eV [3]. The simulated cases comprise different starting angles for electrons: 30°, 45°, 60°, 90° and different biasing voltage: 60 V, 100V, 200V. The adopted model represents the accelerator and STRIKE inside the vacuum vessel, distanced by 1 m from each other. Both accelerator and calorimeter are 0.8 m wide, 1.6 m tall. Figure 1 represents the electric field at 200 V calorimeter biasing voltage:

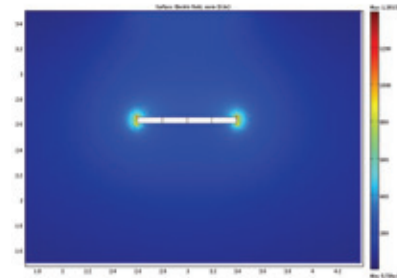


Figure 1: Zoom of electric field intensity around the calorimeter at 200 V of biasing voltage

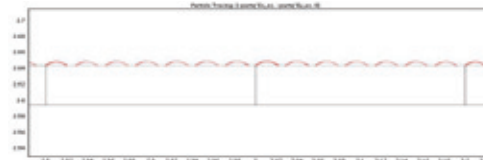
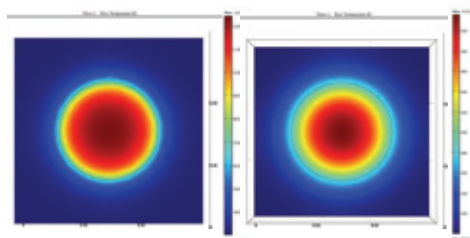


Figure 2: Zoom of electrons trajectory at 200 V and 45° starting angle

and Figure 2 secondary electrons trajectory at 200 V and 45° starting angle. The best choice seems 200 V, which gives a worst-case range of 21 mm and should be sufficient if the beamlets are in their nominal positions.

For the heat flux analyses various materials, with linear and non-linear characteristic parameters (thermal conductivity, specific heat), have been considered for comparison: graphite and Carbon Fibre Composite (CFC) (MFC-1A by Mitsubishi, like JET instrumented calorimeter [4]; 2602ZV by SGL CARBON GROUP and 1501G by SGL CARBON GROUP). The two following figures show a comparison between material in the same condition: 20 mm model thickness, 20 MW/m<sup>2</sup> power load and 1 s pulse duration; observation performed when heat load ends. Figure 3 shows the beamlet pattern of 2602ZV and maximum temperature reached: 1241 K for the front side (left) and 515 K at the rear side (right).



**Figure 3:** Front (on the left) and back (on the right) side of 2602ZV

Figure 4 shows the beamlet pattern of MFC1-A and maximum temperature reached: 990K for the front side (left) and 577 K at the rear side (right).

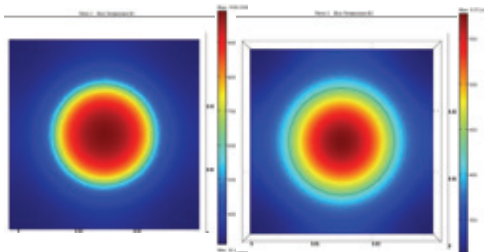


**Figure 4:** Front (on the left) and back (on the right) side of MFC1-A

From surface temperature results and material characteristic, MFC1-A and 20 mm thickness is the data for future simulations.

### 3.2 Assessment of calorimeter position

Thermal analyses have shown that high temperatures can be reached on the calorimeter surface directly exposed to the beam. In this section different calorimeter positions will be compared. The effect of the beam on the

calorimeter surface depends on several parameters: horizontal and vertical deflection of the beamlets ( $\alpha$ , angle for vertical displacement, and  $\beta$ , angle for horizontal displacement), beamlet width in x and y directions ( $\sigma_x, \sigma_y$ ), divergence along x and y directions ( $\delta_x, \delta_y$ ), distance between accelerator and calorimeter, angle ( $\gamma$ ) of the normal to the calorimeter surface with respect to the beam direction. Only a quarter of beamlet group is simulated based on existing symmetries. In these cases the beam is approximated with a Gaussian distribution. Figure 5 shows the simulated cases:

Case	Vertical deflection (mrad)	Horizontal deflection (mrad)	Beamlet width (mm)	$\alpha$ (deg)	$\beta$ (deg)	E (MW/m <sup>2</sup> )	$\gamma$ (deg)	Distance between calorimeter and target (m)
100	0	0	0.16	0	0	20	0	1
105	0	0	0.16	0	0	20	0	1
110	0	0	0.16	0	0	20	0	1
115	0	0	0.16	0	0	20	0	1
120	0	0	0.16	0	0	20	0	1

**Figure 5:** Parameters of simulated cases

The dimensions of the modelled system are:  $(0.396/2) \times (0.16/2)$  for flux perpendicular to the calorimeter;  $(0.396/2) \times (0.32/2)$  for an angle of 60° with respect to the flux. The model does not include radiation from the sample: after heat load ends, all external surfaces of the samples are thermally insulated. Figure 6 and Figure 7 show the comparison between angled and orthogonal cases, with the same parameter: 5 s pulse duration and observation when heat load ends, 3 mrad divergence, 1 m from the accelerator.

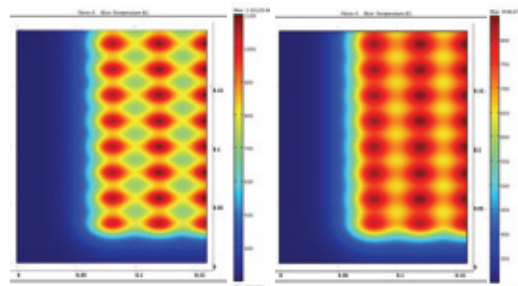


**Figure 6:** Angled cases, maximum superficial temperature in the front (left) is 1100 K and at the rear side (right) is 848 K

From the analyses presented herein, it can be concluded that the calorimeter should be angled with respect to the beam direction. An angle of 60 degrees between the beam direction and the normal to the calorimeter surface should be sufficient to avoid too high superficial

temperature, to allow 5 s pulses and at the same time to provide a good IR cameras image.

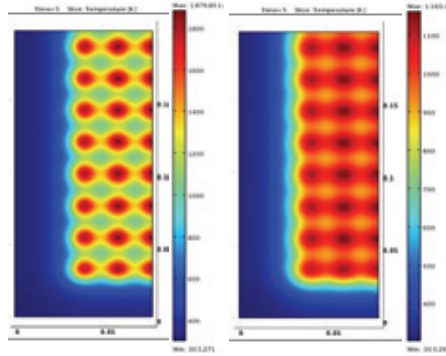


**Figure 7:** Orthogonal cases, maximum superficial temperature in the front (left) is 1880 K and at the rear side (right) is 1160 K

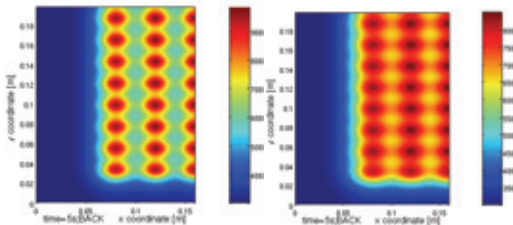


**Figure 8:** Comparison between cases at different distances from the accelerator

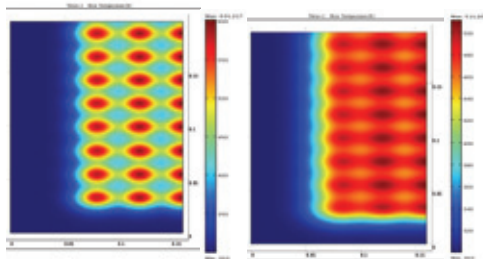


**Figure 9:** Comparison between cases at different divergence value: 3 mrad left and 5 mrad right

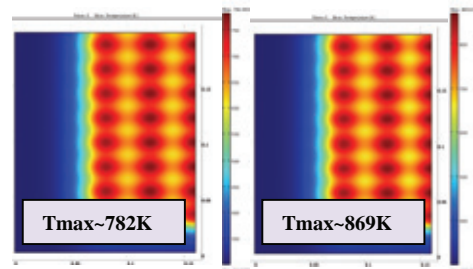
### 3.3 Measurements of divergence

Figure 8 compares cases with the same parameters at two different distances from the accelerator. From the comparison between this two thermal pattern divergence can be calculated. Figure 9 compares cases in which the only difference is the divergence value: superficial temperature is 600 K for 3 mrad divergence (left) and decreases to 510 K for 5 mrad divergence (right).

Both these figures show the sensitivity of the thermal pattern to the beam divergence, so, from the simulation results it can be concluded that the divergence can be measured.

### 3.4 Uniformity

Cases with  $-15\%$  and  $+5\%$  power per beamlet are compared to the reference case:



**Figure 10:** Temperature with  $-15\%$  power per beamlet is 782 K (left) and temperature with  $+5\%$  power per beamlet is 869 (right)

Figure 10 shows about 20 K temperature variation every 5 % of power per beamlet variation, with respect to the reference case (848 K); such variation should be appreciated by IR cameras as clearly highlighted by the simulation results.

### 3.5 Assessment of sensitivity of beam deflection

The purpose of this analysis is to assess the possibility of using the calorimeter for the assessment of the beamlet misalignment. The beam is approximated with a Gaussian distribution. The adopted numerical model represents only half of the calorimeter beamlet group based on the existing symmetries. The dimensions of the modelled system are:  $(0.396/2) \times (0.32) \text{ m}^2$ . Vertical misalignment is negligible because all beamlet groups can be maintained within each tile so the uniformity parameter is not affected and measurable. Horizontal misalignment is instead considered  $\pm 2.5 \text{ mrad}$  according to the particle trajectory simulation results.

The analyses presented in Figure 11 show that STRIKE should be able to provide information also about the effectiveness of the strategies applied to the reduction of the deflection of negative ion beamlets: indeed, the simulations

display that the beamlets are clearly identified in the thermal images.

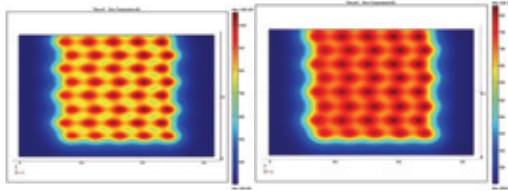


**Figure 11:** Front (left) and rear (right) thermal patterns in case of  $\pm 2.5$  mrad misalignment

### 3.6 Thermal simulation with radiation

Three different cases have been studied: (1) after the application of the flux, all faces of the tile are thermally insulated; three consecutive 5 s loads have been applied; (2) after the application of the flux, all faces of the tile are thermally insulated; at all times the face opposite the one hit by the beam radiates towards a surface at 300 K; four consecutive 5 s loads have been applied; (3) after flux application, all tile faces are thermally insulated; at all times the face opposite the one hit by the beam radiates towards a surface at 300 K; three consecutive 10 s loads have been applied. Figure 12 shows front and rear side temperatures reached at the end of the third beam pulse in case (3): about 1800 K for the front and about 1400K for the back. Figure 13 shows the temperature profile in the centre of a beamlet in the middle of the beamlet group for the three cases. It can be noticed that up to 10 s, cases (1) e (2) (chain and red lines respectively) show no appreciable difference. This suggests that radiation does not affect the measurement in short times in that location, and can be neglected in the deduction of the heat flux from the temperature pattern. Case (3) exhibits a larger temperature (violet line) due to the larger duration of the beam pulse (10 s instead of 5 s). In Figure 14 the temperature at the border of the tile is displayed for all cases. This point is important due to the vicinity to the stainless steel frame. The temperature keeps increasing without radiation; conversely, with radiation, the difference between the temperatures measured just before successive beam pulses decreases with the number of pulses and the temperature tends to saturate between two values. The maximum temperature reached in this position is sustainable by the stainless steel frame of the calorimeter.

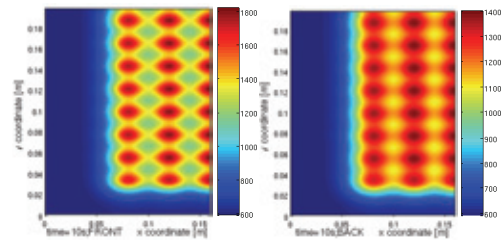


**Figure 12:** Front (left) and rear (right) sides in correspondence to the end of the third 10 s beam pulse, case (3)

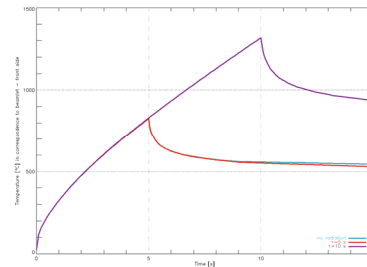


**Figure 13:** Front temperature profile in correspondence of first beam pulse in the center of the central beamlet

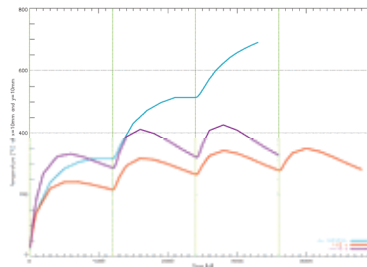


**Figure 14:** Temperature at the border with several subsequent beam pulses

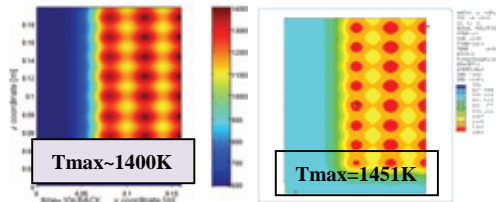
These results provide the operational range of IR cameras, suggest a duty cycle of 10 s pulse duration and 1200 s between pulses and exclude the necessity of an active cooling system.

### 4. Comparison with Ansys

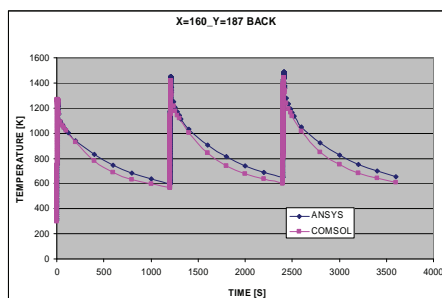
In selected cases, a comparison has been performed between the present results and an analogous simulation obtained by the ANSYS code. Figure 15 shows that the maximum back side temperature worked out by Comsol and Ansys are quite the same:

Figure 16 shows the comparison of the temporal trend of the back side temperature in Comsol and Ansys in the center of the central beamlet.

From the figures presented herein it can be concluded that the results of Ansys and Comsol match.



**Figure 15:** Thermal pattern comparison between Comsol and Ansys



**Figure 16:** Temporal trend of back side temperature in Comsol and Ansys in the center of the central beamlet

## 5. Conclusions

Several thermal and electrostatic simulations, and a comparison with another analysis code have been done to assess the feasibility and also the working conditions of the diagnostic calorimeter for the neutral beam injector for ITER, which aims at measuring the beam characteristics.

The project of the system has begun on the basis of the simulation results, which concerned definitive decisions like: tile dimensions, reference material (1D-CFC), 60° exposure angle, two measurement axial distances (about 1m and 0.5 m from the accelerator), two positions to permit long operation of the source (open, close), absence of an active cooling system, tiles electrically insulated, biasing voltage (200 V), 10 s pulse duration and 1200 s time between pulses, observation at the rear side.

## 6. References

1. P. Sonato *et al.*, The ITER full size plasma source design, *Fusion Eng. Des.* **84**, 269 (2009)

2. A. Rizzolo *et al.*, Design and analyses of a one-dimensional CFC calorimeter for SPIDER beam characterization, submitted to *Fusion Eng. Des.*

3. G. Fubiani *et al.* Modelling of secondary emission processes in the negative ion based electrostatic accelerator of ITER, *Phys. Rev. STAB* **11**, 014202 (2008)

4. D. Čirić *et al.*, Beam profile measurements using a unidirectional CFC-target and infrared imaging, *Fusion Technol.* 827 (1994)

## 7. Acknowledgements

This work was set up in collaboration and financial support of Fusion for Energy.